COHERENT INSTABILITY THRESHOLDS AND DYNAMIC APERTURE WITH OCTUPOLES AND NONLINEAR SPACE-CHARGE IN THE SIS100 SYNCHROTRON

Vladimir Kornilov, Oliver Boine-Frankenheim, GSI, Darmstadt, Germany
Valery Kapin, GSI, Darmstadt, Germany; ITEP, Moscow, Russia

Abstract

Octupole magnets can be used as a passive cure against transverse collective instabilities. The octupole field creates a betatron frequency spread due to amplitude-dependent tune shift and thus enhances Landau damping. The drawback is the reduction of the dynamic aperture (DA). Ultimately, a balance between collective damping and DA must be found. Here we analyse the transverse coherent instability thresholds in SIS100 [1] with octupoles and nonlinear space-charge taken into account. As the major impedance source at low frequencies, the resistive wall is considered. A coasting beam is assumed, which results in a conservative stability estimation. On the other hand, we simulate the DA of the SIS100 lattice using the MADX code, with systematic multipole errors, random multipole errors, and closed-orbit errors taken into account.

COHERENT STABILITY

Landau damping due to the momentum spread [2] can be characterized by the efficient betatron tune spread,

$$\delta Q_\xi = |\eta(n - Q_0) + Q_0\xi|\,\delta_p\ ,$$

for the slow waves $f = (n - Q_0)f_0$, which describe the unstable spectrum in a coasting beam. Here $f_0 = \omega_0/2\pi$ is the revolution frequency, Q_0 is the bare betatron tune, $\xi = d\ln Q/d\ln p$ is the chromaticity, η is the slip factor and $\delta_p = \delta p/p$ is the rms momentum spread.

Beam stability can be enhanced by other sources of the betatron tune spread, which can be of an intrinsic origin (space charge) or external (as octupoles). In both of these cases an amplitude-dependent tune shift is induced. In this situation, the following dispersion relation [3] for coherent oscillations in the vertical plane (y) can be used,

$$\int \frac{\Delta Q_{\rm coh} - \Delta Q_{\rm sc}}{\Omega/\omega_0 + \Delta Q_{\rm ex} + \Delta Q_{\rm sc}} J_y \frac{\partial\psi_\perp}{\partial J_y}\psi_p \mathrm{d}J_x\mathrm{d}J_y\mathrm{d}\hat{p} = 1 \quad (1)$$

Here $\Delta Q_{\rm sc}(J_x, J_y)$ is the space-charge tune shift, the frequency shift we define as $\omega = (n - Q_0)\omega_0 + \Omega$, J_x and J_y are the transverse action variables, $y = \sqrt{2J_y\beta_y}\cos\phi_y$, $\psi_\perp(J_x, J_y)$ is the transverse distribution, $\hat{p} = \Delta p/p$ is the momentum offset and $\psi_p(\hat{p})$ is the corresponding distribution, the normalization is $\int \psi_\perp\psi_p \mathrm{d}J_x\mathrm{d}J_y\mathrm{d}\hat{p} = 1$. $\Delta Q_{\rm coh}$ is the coherent tune shift which is induced by a facility impedance. $\Delta Q_{\rm ex}$ includes external incoherent tune shifts, in our case due to octupole lenses and due to the chromaticity effect,

$$\Delta Q_{\rm ex}(J_x, J_y, \hat{p}) = \Delta Q_{\rm oct}(J_x, J_y) + \Delta Q_\xi(\hat{p})\ . \quad (2)$$

Beam stability with nonlinear space charge was also studied in [4, 5], applicability of Eq. (1) was discussed in [6, 7], a comparison with numerical simulations was made in [6].

In this work we assume a Gaussian profile for the transverse beam distribution and take into account a two-dimensional tune shift dependence [7, 8]. For the SIS100 U^{28+} beam [9] at the injection energy, the space charge tune shift of the rms-equivalent K-V beam is $\Delta Q_{\rm lin} = -0.033$, the strongest tune shift for the Gaussian distribution is $\Delta Q_{\rm max} = 2\Delta Q_{\rm lin}$.

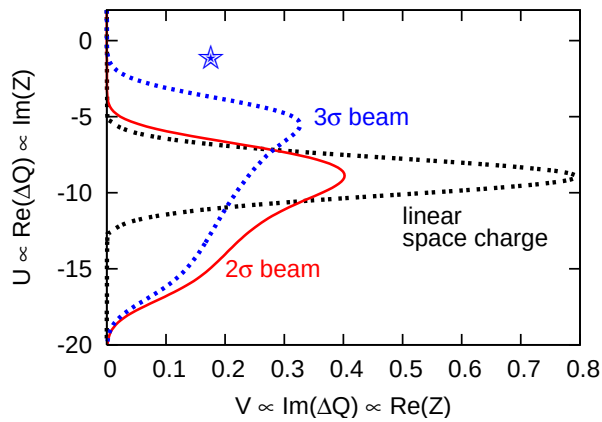

Figure 1: Stability diagrams for a combination of δ_p with nonlinear space charge for a SIS100 coasting beam.

Solutions of Eq. (1) are presented in the form of stability diagrams which show the contour level for $\mathrm{Im}(\Omega) = 0$ in the normalized impedance plane $V + iU = -i\Delta Q_{\rm coh}/\delta Q_\xi$. The stable areas are the regions enclosed by the curves and by the $U-$axis. Figure 1 presents stability diagrams for a combination of the momentum spread with space charge. The black line corresponds to a constant space-charge tune shift, while the red and the blue lines compare beam stability for truncations at 2σ and at 3σ of the transverse distribution. The star indicates the impedance in SIS100 [9] at $Q = 1 - Q_{\rm f}$, where $Q_{\rm f}$ is the fractional part of Q_0. At this low frequency the impedance is dominated by the resistive wall impedance [9] and by the image charges.

From Fig. 1 we conclude that, firstly, Landau damping due to the momentum spread does not provide transverse stability in SIS100. This is due to the loss of Landau damping given by space charge, the nonlinear part of which enhances stability though. Secondly, for a transverse Gaussian profile, tails of the distribution are important for a stability analysis, which is then sensitive to the truncation. We choose a truncation at 2.5σ in the following analysis.

The field of an octupole with the strength $K_3 = g/B\rho$ is

$$B_x = \frac{g}{6}(-y^3 + 3x^2y), \quad B_y = \frac{g}{6}(x^3 - 3x^2y) \ ,$$

the resulting vertical tune shift is given by

$$\Delta Q_{\rm oct} = \Big(\int \frac{K_3\beta_y^2}{16\pi}{\rm d}s\Big)J_y - \Big(\int \frac{K_3\beta_x\beta_y}{8\pi}{\rm d}s\Big)J_x \ , \quad (3)$$

and for the horizontal plane correspondingly. As a result of taking into account octupole magnets in the configuration [10] which is foreseen in the SIS100 lattice, we obtain stability diagrams shown in Fig. 2. Three different octupole strengths are presented, for $K_3 = 50\,{\rm m}^{-4}$ the stability boundary reaches the impedance. Note that the polarity $K_3 < 0$ is disadvantageous for beam stability [6].

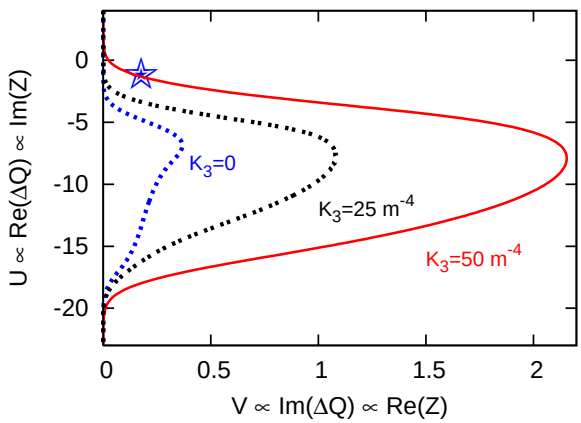

Figure 2: Stability diagrams as given by Eq. (1) for a combination of octupoles with δ_p and with nonlinear space charge for a SIS100 coasting beam.

DYNAMIC APERTURE SIMULATIONS

Twelve identical octupoles in the SIS100 lattice are considered. One half of them is located near the maxima of β_x, the other half is intended for the vertical plane. The maximum gradient in lenses is 2000 T/m^3 and the effective length is 0.75 m, at the injection energy for U^{28+} ions this corresponds to the octupole coefficient $K_3 = 109\,{\rm m}^{-4}$. In this work, MAD-X [11] simulations for four configurations $K_3 = \pm 100\,{\rm m}^{-4}$ and $K_3 = \pm 50\,{\rm m}^{-4}$ are made for comparisons. Firstly, we check the tune spread due to octupoles. The linear SIS100 lattice with the octupoles is considered. Figure 3 shows the footprints obtained for the octupole strength $K_3 = 50\,{\rm m}^{-4}$ and maximum emittances $\epsilon_x = \epsilon_y = 48$ mm mrad. The footprint calculated using Eq. (3) is given in the upper plot, while the lower plot shows a result of a MAD-X simulation.

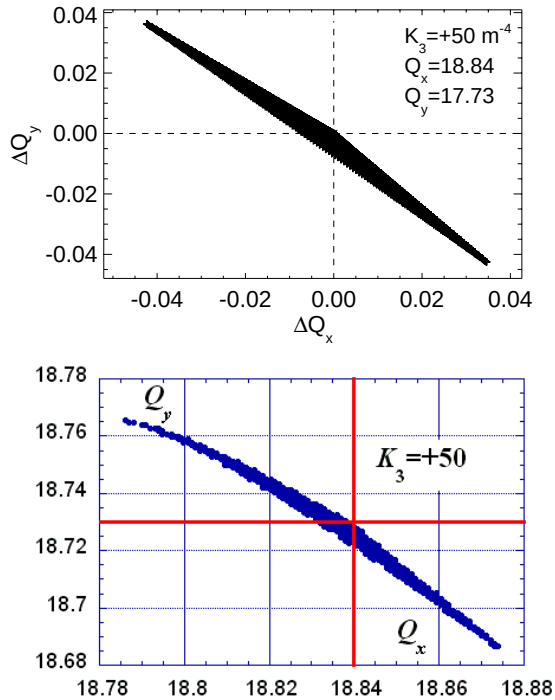

Figure 3: Tune footprint for a SIS100 lattice with octupoles obtained analytically (upper plot) and in a MAD-X simulation (lower plot).

Multipole coefficients for SIS100 superconducting dipoles and quadrupoles from [10, 12] have been assumed for the systematic errors. The random errors are simulated according to the Gaussian distribution at the level $\pm 30\%$ of the systematic errors. For the closed orbit distortion, misalignment errors of quadrupoles are assumed to be the main error source [12]. A set of SIS100 lattices with the rms closed orbit distortion close to $\langle x_{\rm CO}\rangle$=1.4 mm and $\langle y_{\rm CO}\rangle$=1 mm has been generated.

To evaluate the dynamic aperture (DA), particles with different $x_{\rm in}, y_{\rm in}$ but $x'_{\rm in} = y'_{\rm in} = 0$ are tracked for a number of turns. Normally, 10^3 turns correspond to the so-called short-term DA. According to the applied DA-algorithm, the minimum value for the invariant sum $(\epsilon_x + \epsilon_y)$ is calculated for every boundary trajectory over all turns. The intersection of every parental ray $(\epsilon_y/\epsilon_x)_{\rm in}$ with the line $(\epsilon_x + \epsilon_y)_{\rm min}$ provides a DA-boundary point on the corresponding parental ray. The ensemble of such points forms the DA-boundary curve on the emittance plane. Details of this DA-algorithm are given in [10]. In order to quantify a DA boundary, the minimum $\epsilon_r^{\rm min}$ and average $\langle\epsilon_r\rangle$ radii for these DA curves are used.

An example for our DA simulations with the MAD-X code is shown in Fig. 4. Here, a lattice with the systematic

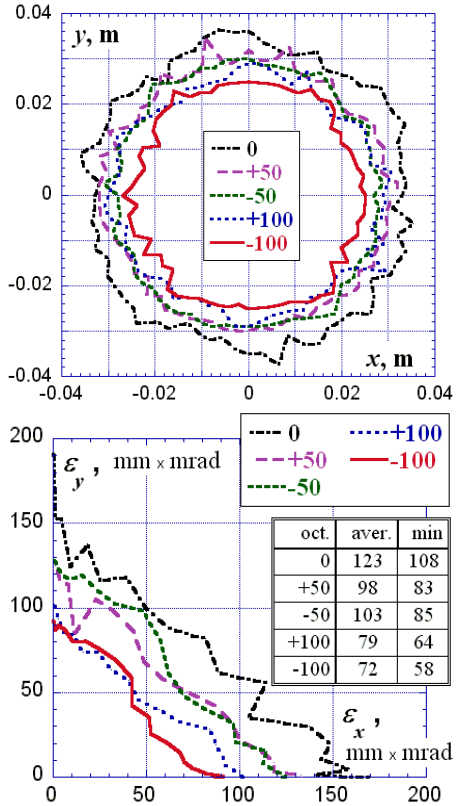

Figure 4: DA simulations: boundary of the stability domain for a SIS100 lattice with systematic errors and random errors for different octupole strengths.

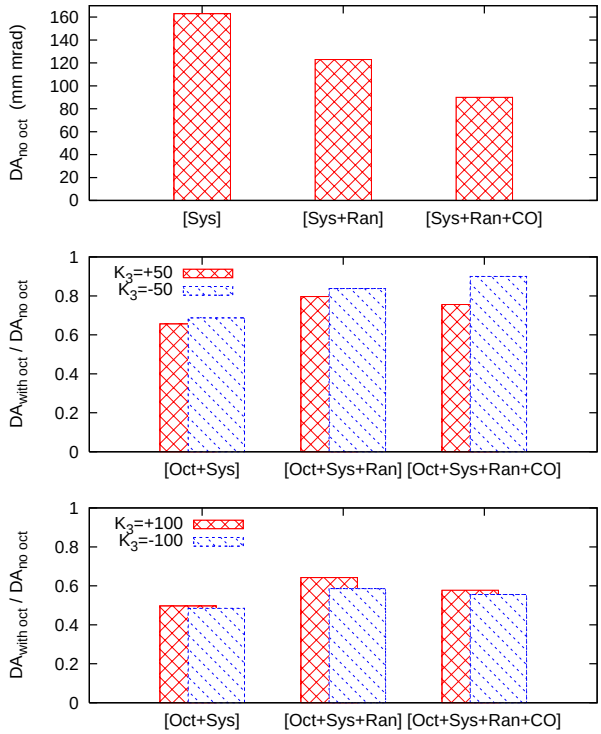

Figure 5: Summary for DA simulations: $\langle \epsilon_r \rangle$ for different lattices and octupole strengths.

errors and with the random errors is considered. Stability boundaries are shown on the (x, y) plane (upper plot) and on the emittance plane (lower plot). For $K_3 = \pm 100\,\mathrm{m}^{-4}$, the average and the minimal DA-emittances essentially reduced by approximately 40%, while for the moderate octupole $K_3 = \pm 50\,\mathrm{m}^{-4}$ this reduction is about 15%.

CONCLUSIONS

Transverse stability of a SIS100 coasting beams as a conservative estimation has been evaluated, with nonlinear space charge, momentum spread, and realistic SIS100 octupoles taken into account. Landau damping due to momentum spread does not provide transverse stability. Our analysis suggests that the octupole magnets at strength $K_3 = 50\,\mathrm{m}^{-4}$ should make an important contribution into beam stability.

Results of our DA simulations summarized in Fig. 5, where average emittances for the different cases are presented. Nonlinearities are denoted as following: "Sys" is for the lattice with the systematic errors only, "Ran" indicates random multipole errors, and "CO" is the label for the closed-orbit errors. These results suggest that octupoles at the maximum strength can significantly (up to approx. 40% related to other nonlinearity sources) reduce the dynamic aperture in SIS100, while $K_3 = 50\,\mathrm{m}^{-4}$ octupoles can cause an approx. 20% reduction. The role of the octupole nonlinearity seems to decrease if one includes more error sources and thus makes the analysis more realistic.

REFERENCES

[1] FAIR Baseline Tech. Report 2006: http://www.gsi.de/fair/reports/btr.html

[2] A. Hofmann, CERN Acc. School, Rhodes, Greece, 20 Sep - 1 Oct 1993, (CERN 95-06 v.1, p. 275)

[3] D. Möhl, H. Schönauer, Proc. IX Int. Conf. High Energy Acc., Stanford, 1974, p. 380 (1974)

[4] M. Blaskiewicz, Phys. Rev. ST Accel. Beams **4**, 044202 (2001)

[5] E. Métral, F. Ruggiero, Proc. EPAC2004, Lucerne, Switzerland, 5-9 July 2004, p. 1897 (2004)

[6] V. Kornilov, O. Boine-Frankenheim, and I. Hofmann, Phys. Rev. ST Accel. Beams **11**, 014201 (2008)

[7] A. Burov and V. Lebedev, Phys. Rev. ST Accel. Beams **12**, 034201 (2009)

[8] *Handbook of Accelerator Physics and Engineering*, edited by A.W. Chao and M. Tigner (World Scientific, 1999)

[9] V. Kornilov, O. Boine-Frankenheim, I. Hofmann, Acc-Note-2008-006, GSI Darmstadt (2008)

[10] V. Kapin and V. Kornilov, Acc-Note-2009-006, GSI Darmstadt (2009)

[11] MAD-X Code: http://mad.home.cern.ch

[12] FAIR Technical Design Report SIS100, pp. 39–49, GSI, Darmstadt, (2008)